BMC Chemistry

RESEARCH

Open Access

Molecular hydrogen mitigates traumatic brain injury-induced lung injury via NLRP3 inflammasome inhibition

Lingling Liu[1,2], Shuzhi Wang[3], Lianhao Jiang[1,2], Jiwei Wang[2,4], Jun Chen[1,2], Hongtao Zhang[1,2*] and Yuanlin Wang[5*]

Abstract

Introduction Hydrogen gas has demonstrated significant antioxidant and anti-inflammatory properties, suggesting potential therapeutic benefits in TBI.

Methods We subjected to controlled cortical impact in mice to construct TBI model. They received an intraperitoneal injection of MCC950, a selective NLRP3 inhibitor, at 10 mg/kg 30 min before TBI. Inhalation of 2% H_2 is adopted in TBI mice for 60 min, starting 1 and 6 h post-TBI. 24 h after H_2 inhalation, we extracted tissues and analyzed injury related changes. The H_2 levels in arterial and venous were tracked after inhalation. Lung tissue was examined for histopathological changes and apoptosis using H&E and TUNEL assays. The total protein in the BALF, oxygenation index, lung wet-to-dry weight ratio, and lung MPO activity were measured to evaluate the severity of TBI-induced lung injury. Protein and mRNA levels of NLRP3, ASC, Caspase-1, IL-18, and IL-1β in the lung tissue were quantified using western blotting and quantitative PCR. The expression changes and distribution status of NLRP3 and Caspase-1 were examined by immunofluorescence and immunohistochemistry staining.

Results Significant lung injury at 24 h post-TBI got significantly reduced by treatment of 2% H_2. TBI activated the NLRP3 inflammasome, increasing NLRP3, ASC, and caspase-1 levels, to lead to higher IL-1β and IL-18 secretion in the lungs. Blocking NLRP3 reduced lung damage from TBI, and its combination with 2% H_2 provided better protection than either treatment alone.

Conclusions 2% H_2 can protect against TBI-induced lung injury by inhibiting NLRP3 inflammasome activation, thereby alleviating inflammation and inhibiting apoptosis.

Keywords Hydrogen gas, Traumatic brain injury, Lung injury, NLRP3 inflammasome

*Correspondence:
Hongtao Zhang
zhanght80@126.com
Yuanlin Wang
wyl1996@tmu.edu.cn
[1] Department of Anesthesiology, Tianjin Huanhu Hospital, NO. 6 Jizhao Road, Jinnan District, Tianjin 300350, China
[2] Tianjin Key Laboratory of Cerebral Vascular and Neurodegenrative Diseases, Tianjin 300350, China
[3] Department of Cardiac Function, Tianjin Thoracic Hospital, Tianjin Institute of Cardiovascular Diseases, Tianjin 300222, China
[4] Department of Neurosurgery, Tianjin Huanhu Hospital, Tianjin 300350, China
[5] Department of Anesthesiology, Tianjin Institute of Anesthesiology, Tianjin Medical University General Hospital, No. 154 Anshan Rd, Heping District, Tianjin 300052, China

Introduction

Among TBI-related complications, secondary acute lung injury is the most common and important complication [1]. Over 50% of individuals with isolated severe traumatic brain injury (TBI) develop acute lung injury [2].There are two frequent extracranial complications of TBI, respectively acute lung injury (ALI) and acute respiratory distress syndrome (ARDS) [3]. Meanwhile, lung injury also could be seen as a key predictor of mortality in TBI, and TBI patients with ARDS has a mortality rate of 30–40% [4]. The primary risk factors for ALI or ARDS following TBI include pneumonia, sepsis, and aspiration of gastric contents [5]. Inflammatory mediators released from damaged brain tissue lead to a systemic inflammatory response in the lungs, which is a basic cause of ALI after TBI [6]. Thus, reducing excessive pulmonary inflammation is critical for improving outcomes in TBI patients.

Hydrogen gas (H_2) has been reported to treat various diseases in animal studies and clinical trials [7]. Due to it owns special antioxidant and anti-inflammatory abilities, molecular hydrogen treatment is believed to be of potential for a range of neurological disorders, for instance traumatic brain injury, Alzheimer's disease, depression, anxiety, ischemic stroke, and multiple sclerosis [8]. Our researches demonstrated that inhalation of 2% H_2 significantly protect brain against injury and cognitive dysfunction in septic mice by regulating neuroinflammation, decreasing oxidative stress, and neuronal apoptosis [9]. Additionally, H_2 has been also found to alleviate lung and intestinal injuries induced by sepsis by mitigating inflammation and oxidative stress [10, 11].

NLRP3 protein is a cytosolic pattern related recognition receptor, helping detect microbial motifs, endogenous danger signals, and stress signals. Once activated, NLRP3 assembles a multiprotein inflammasome complex, enables to activate Caspase-1 enzyme and facilitate the release of pro-inflammatory cytokines such as IL-1β and IL-18 [12]. Some studies have shown that inhibiting chronic NLRP3 activation after TBI can prevent long-term brain dysfunction by regulating neuroinflammation and preventing apoptosis [13]. Furthermore, H_2 inhalation has been found to participate with the ROS/NLRP3 axis to alleviate inflammation and oxidative stress in rats following subarachnoid hemorrhage (SAH), being helpful for improving neurobehavioral outcomes [14].

Our study planned to investigate the role of H_2 in alleviating TBI-inducing acute lung injury in mice and explore its potential therapeutic mechanisms through inhibition of the NLRP3 signaling pathway.

Materials and methods

Animals experiment design

Male C57BL/6 J mice (6–8 weeks, 20–25 g) were acquired from the Laboratory Animal Center at the Military Medical Science Academy in Beijing, China. All experimental got approved from the Animal Ethical and Welfare Committee of Tianjin Huanhu Hospital, Tianjin, China. Mice were kept in controlled environment with regulated temperature and humidity. Euthanasia anesthesia of mice using inhalation of sevoflurane according to ethical requirements.

The study randomaly included five experimental groups: sham, TBI, TBI + M, TBI + H_2, and TBI + H_2 + M. The experimental design and procedures are outlined in Fig. 1A. MCC950, a selective NLRP3 inhibitor (Thermo, USA), was prepared by dissolving it in sterile phosphate-buffered saline (PBS) at a concentration of 10 mg/ml. For the TBI + M and TBI + H_2 + M groups, MCC950 was administered intraperitoneally at a dose of 10 mg/kg, 30 min prior to TBI. The dose of MCC950 was selected based on previous studies [15]. Mice in the TBI + H_2 and TBI + H_2 + M groups were adapated to 2% H_2 inhalation for 60 min, beginning 1 h and 6 h after TBI, respectively.

Experiment 1: H_2 concentration in arterial and venous blood was detected in mice of each group (n = 6). Catheterization via femoral artery and vein puncture in mice, the arterial blood and venous blood were collected (10μL each time) for detection of H_2 concentration at 0, 10, 20, 30, 45 and 60 min after starting H_2 inhalation and at minute 5, 15, 30 and 45 after the termination of H_2 inhalation, respectively [16]. The grouping method was the same as described above.

Experiment 2: The total protein in the BALF, oxygenation index, lung wet-to-dry weight ratio, and lung MPO activity were measured to evaluate the severity of TBI-induced lung injury (n = 6). The grouping method was the same as described above.

Experiment 3: The histopathology changes and apoptosis in lungs among all groups were measured to affirm effects of 2% H_2 inhalation on TBI mice. Mice were divided into different groups and given with certain treatment. Sevoflurane was used to anesthetize mice and lung tissues were collected at 24 h after operation (n = 6). The tissues were fixed in 4% paraformaldehyde for 24 h, embedded in paraffin, and then sectioned into 5 μm thick slices for staining.

Experiment 4: Mice were divided into different groups as described above and given with certain treatment. Lung tissues were collected at 24 h after operation with same method as described above to detect the protein and mRNA levels. Protein levels of NLRP3, ASC, Caspase-1, IL-18, and IL-1β in the lung tissue were quantified using western blotting (n = 3). In addition, mRNA

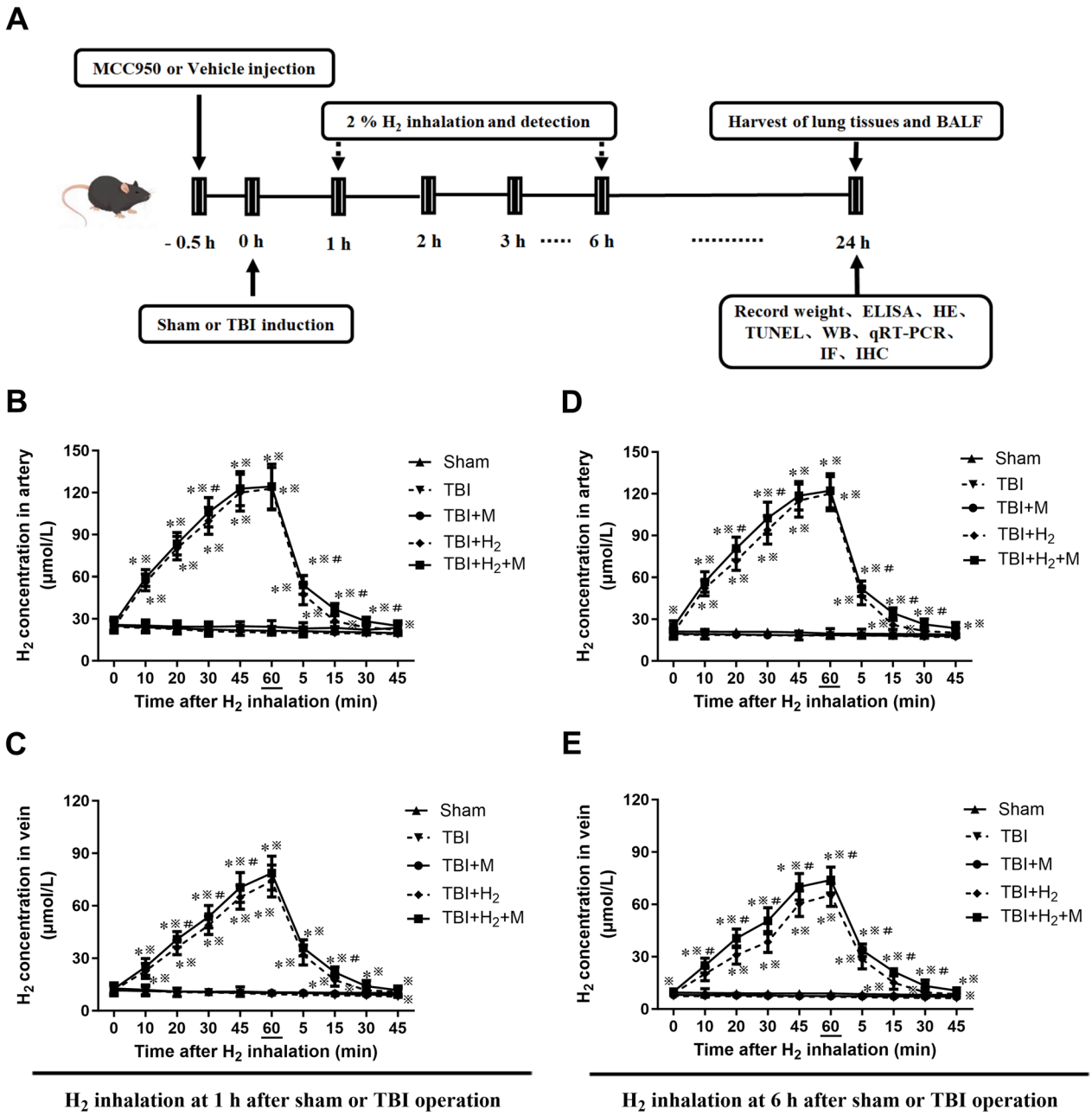

Fig. 1 H_2 concentration was detected after 2% H_2 inhalation, initiated at both 1 and 6 h post-TBI or sham operation, respectively. **A** Experimental flowchart. **B**–**E** H_2 concentrations of arterial and venous at 0, 10, 20, 30, 45, and 60 min after H_2 inhalation start, and at 5, 15, 30, and 45 min time point after the termination of H_2 inhalation in all groups of mice. Values are presented as mean ± standard deviation (n = 6).*P < 0.05 versus Sham group; ※P < 0.05 versus TBI group; #P < 0.05 versus TBI + H_2 group

levels of NLRP3, ASC, Caspase-1, IL-18, and IL-1β in the lung tissue were quantified using quantitative PCR (n = 5).

Experiment 5: The expression changes and distribution status of NLRP3 and Caspase-1 were examined by immunofluorescence and immunohistochemistry staining with the prepared lung tissue slices as above (n = 5).

Construction of TBI model

TBI was realized using a controlled cortical impact device (Custom Design & Fabrication, Sandston, VA, USA) [17]. Mice were anesthetized initially with 2% sevoflurane and maintained under 1–2% sevoflurane. They were positioned on a stereotaxic frame, ensuring that the line between the right eye and ear was parallel to the

horizon. A 4.0 mm craniotomy was performed on the parietal bone, 2.0 mm lateral to the midline and 2.0 mm posterior to the coronal suture. The controlled cortical impactor device was set to impact the brain at a velocity of 4.5 m/s, retention time of 200 ms, and penetration depth of 1.8 mm. The scalp incision was then sutured closed after the procedure.

H_2 inhalation

We introduced hydrogen gas into the chamber via TF-1 gas flowmeter (YUTAKA Engineering Corp, Tokyo, Japan) and air were mixed, at a average flow rate of 4 L/min. The H_2 input was continuously monitored using a Hy Alerta Handheld Detector (Model 500, Valencia, CA) to maintain a steady concentration of 2% throughout the treatment. Carbon dioxide was removed from the chamber using Baralyme.

H_2 concentration detection in arterial and venous

We detected H_2 concentration in both arterial and venous using hydrogen sensor (Unisense, Denmark). Blood samples were collected at the following intervals: 0, 10, 20, 30, 45, and 60 min after the initiation of H_2 inhalation, and 5, 15, 30, and 45 min after the inhalation was discontinued.

BALF total protein assay

We collected bronchoalveolar lavage fluid from mice using a method previously described [18]. The airways were lavaged with 1.0 mL of phosphate-buffered saline (PBS, pH 7.4). The lavage fluid was centrifuged at 1500 *g* for 10 min, and collected the supernatant. BALF total protein concentration was assessed using a protein assay kit from Bio-Rad Laboratories (Hercules, CA, USA).

Lung oxygenation index analysis

Lung oxygenation got evaluated using the PaO_2/FiO_2 ratio. Twenty-four hours after TBI or sham surgery, mice were anesthetized and intubated with a 20-gauge catheter. They were placed on mechanical ventilation with the following parameters: 100% FiO_2, a tidal volume of 7 mL/kg, and a respiratory rate of 120 breaths/min. The mice were ventilated for 20 min before arterial blood was drawn from the carotid artery for gas analysis using a GEM Premier 3000 gas analyzer (Instrumentation Laboratory, Milan, Italy).

Lung W/D weight ratio

All mice were anesthetized and euthanized to collect the lungs. The lungs were weighed to determine the wet weight, then dried in an oven at 80 °C for 24 h to measure the dry weight. The lung wet-to-dry weight ratio was calculated to evaluate the severity of pulmonary edema.

Lung MPO activity assay

We aimed to detect the MPO concentration in lung tissue. Myeloperoxidase (MPO) activity, a marker of neutrophil infiltration, was assessed in the lung homogenate supernatant using an MPO assay kit (Nanjing Jiancheng Bioengineering Institute, Nanjing, China).

Preparation of lung tissue slices

After 24 h, mice were anesthetized, euthanized, and their lung tissues collected. The tissues were fixed in 4% paraformaldehyde for 24 h, embedded in paraffin, and then sectioned into 5 μm thick slices.

Lung histopathologic score

The lung sections were stained with H&E to evaluate the severity and injury degree of lung injury through histopathological analysis. The features assessed included hyperemia, edema, and so on. All feature were assigned a severity grade ranging from 0 (absent) to 3 (severe). The total score from these assessments was used to determine the overall degree of lung injury [10].

TUNEL staining

Using TUNEL assay to detect apoptotic cells in lung tissues. Apoptotic cells appeared as green fluorescence in the nuclei, while all cell DNA was stained blue with DAPI. The stained sections were examined using a Leica DM 400 B microscope (Leica, Germany).

Western blot assay

Lung samples were collected 24 h after TBI or sham surgery and lysed in radioimmunoprecipitation assay (RIPA) buffer (Beyotime, Jiangsu, China) to extract proteins. Protein concentration was quantified using a bicinchoninic acid (BCA) assay. Equal amounts of protein (50 μg) were separated by SDS-PAGE and transferred to polyvinylidene difluoride (PVDF) membranes (Millipore, Germany). After blocking with 5% nonfat milk for 1 h, the membranes were incubated overnight at 4 °C with primary antibodies against NLRP3 (1:1000, Abcam), ASC (1:1000, Abcam), Caspase-1 p20 (1:1000, Millipore), IL-18 (1:1000, Abcam), IL-1β (1:1000, Abcam), and β-actin (1:2000, Sigma-Aldrich). Following washing, membranes were incubated with horseradish peroxidase-conjugated secondary antibodies (goat anti-rabbit, 1:5000, Invitrogen; goat anti-mouse, 1:5000, Invitrogen) for 1 h at room temperature. Protein bands were visualized using a chemiluminescent substrate (EMD

Millipore), and band intensities were analyzed with Quantity One software (Bio-Rad), with normalization to β-actin.

Quantitative real-time PCR

W collected RNA from lung samples. To quantify mRNA expression levels of NLRP3, ASC, Caspase-1, IL-18, and IL-1β, total RNA was extracted from the tissues using the RNAprep Pure Tissue Kit, and complementary DNA (cDNA) was synthesized through reverse transcription (Takara Bio, Shiga, Japan). Quantitative real-time PCR (qPCR) was then conducted to determine the mRNA levels. The relative expression of the target genes was calculated using the $2-\triangle\triangle CT$ method, with GAPDH mRNA as the internal control. The primers used for amplification were as follows: NLRP3, forward 5′-CCT GGTCTGCTGGATTGTGTGC-3′, reverse 5′-CCTGGT CTGCTGGATTGTGTGC-3′; ASC, forward 5′-CCT GGTCTGCTGGATTGTGTGC-3′, reverse 5-CCT GGTCTGCTGGATTGTGTGC-3′; Caspase-1, forward 5′-CGCATTTCCTGGACCGAGTGG-3′, reverse 5′-GAGGGCAAGACGTGTACGAGTG-3′; IL-18, forward 5′-CGACCGAACAGCCAACGAAT-3′, reverse 5′-GGGTCACAGCCAGTCCTCTT-3′; IL-1β forward 5′-ACAGCAGCATCTCGACAAGAGC-3′, reverse 5′-ACAGCAGCATCTCGACAAGAGC-3′; GAPDH forward 5′-TCAATGAAGGGGTCGTTGAT-3′, reverse 5′-CGTCCCGTAGACAAAATGGT-3′ [19, 20].

Immunofluorescence staining

The tissue sections were deparaffinized and subjected to antigen retrieval using sodium citrate. To block endogenous peroxidase activity, the slides were treated with H_2O_2 for 10 min. After washing with PBS three times, the sections were incubated overnight at 4 °C with an anti-NLRP3 primary antibody (1:100, Abcam, UK). The slides were then rinsed and incubated with an Alexa Fluor 555-conjugated secondary antibody (1:1000, Abcam, UK) for 1 h at room temperature. Nuclei were stained with DAPI for 5 min. NLRP3 expression and distribution were visualized using a Leica DM 400 B microscope (Leica, Germany).

Immunohistochemical staining

After dewaxing, rehydration, and antigen retrieval, all tissue sections were blocked with 5% goat serum for 20 min. Then, they were incubated overnight at 4 °C with an anti-Caspase-1 p20 primary antibody (Millipore, USA). Following incubation, the sections were washed and incubated with a secondary antibody (1:200) for 2 h at room temperature. Diaminobenzidine (DAB) was used for staining, and the nuclei were counterstained with hematoxylin for 5 min. Caspase-1 expression and its distribution were visualized under a Leica DM 400 B microscope (Leica, Germany).

Statistical analysis

All Statistical analyses were performed using GraphPad Prism 10.1.2 software. Data are presented as mean ± standard deviation. For group comparisons, we used one way ANOVA method, followed by Tukey's multiple comparison test. The criteria is set to $P < 0.05$ was considered to be of statistical significance.

Results

H_2 could quickly distribute into the whole body as the H_2 inhalation

In our research, we tracked the blood hydrogen concentration changes. 1 h after initiating 2% H_2 inhalation in sham and TBI mice, hydrogen concentrations in both arterial and venous blood were measured. As shown in Fig. 1B, in the TBI + H_2 and TBI + H_2 + M groups, arterial hydrogen levels rose rapidly after the start of inhalation ($P < 0.05$ compared to the sham and TBI groups at 10, 20, 30, 45, and 60 min), peaking around 45 min. This peak was maintained for an additional 15 min, continuing until the end of the H_2 treatment. The TBI + H_2 + M group owned much higher arterial H_2 concentrations than the TBI + H_2 group at 30 min ($P < 0.05$). After discontinuation of H_2 inhalation, arterial H_2 concentrations dropped rapidly but remained elevated compared to the sham and TBI groups at 5, 15, and 30 min ($P < 0.05$), returning to baseline levels by 45 min. Additionally, the TBI + H_2 + M group showed significantly higher arterial H_2 concentrations at 5, 15, and 30 min post-inhalation cessation compared to the TBI + H_2 group. No significant changes in arterial H_2 levels were observed in the sham, TBI, or TBI + M groups at any time points.

Similarly with arterial blood results, the concentration of molecular hydrogen in the venous blood of the increased after the onset of H_2 inhalation, peaking around 45 min as shown in Fig. 1C. The concentration of H_2 reached its peak 60 min after inhaling hydrogen. Meanwhile, the venous H_2 levels in the TBI + H_2 + M group were significantly higher than in the TBI + H_2 group at 20, 30 and 45 min ($P < 0.05$). After H_2 inhalation ceased, the venous H_2 concentration in both the TBI + H_2 and TBI + H_2 + M groups will rapidly decrease, but could remain elevated compared to the sham and TBI groups at 5, 15, and 30 min ($P < 0.05$). In the end, it will return to baseline by 45 min. What's more, according to our observed results, the TBI + H_2 + M group showed significantly higher venous H_2 concentrations than the TBI + H_2 group at 15 min post-inhalation cessation. No significant

changes in venous H_2 concentrations were observed in the sham, TBI, or TBI + M groups at any of the time points.

As shown in Fig. 1D and E, after 2% H_2 inhalation starting 6 h post-sham or TBI surgery, changes in H_2 concentration of arterial and venous blood both followed a similar pattern to those observed at 1 h post-surgery. However, the venous H_2 concentration in the TBI + H_2 + M group was significantly higher than in the TBI + H_2 group ($P < 0.05$) at 10, 20, 30, 45, and 60 min. In both the TBI + H_2 and TBI + H_2 + M groups, venous blood H_2 levels peaked around 60 min, but the concentrations were higher in the TBI + H_2 + M group compared to the TBI + H_2 group.

2% H_2 treatment and MCC950 decreased total protein concentration in BALF, lung W/D ratio, lung MPO activity and improved PaO_2/FiO_2 ratio in TBI mice

As shown in Fig. 2A–D, in the TBI group 24 h after surgery, increased total protein levels in BALF and decreased PaO_2/FiO_2 ratio, elevated lung W/D ratio, higher MPO activity were all observed. These suggest that lung injury has occurred. 2% H_2 and MCC950 treatments in the TBI + M, TBI + H_2, and TBI + H_2 + M groups reversed these injury performances. Among these, the TBI + H_2 + M group exhibited significantly lower total protein in BALF, reduced lung W/D ratio, and decreased MPO activity, along with a higher PaO_2/FiO_2 ratio compared to the TBI + H_2 group ($P < 0.05$). These results suggest that 2% H_2 treatment effectively mitigates lung injury in TBI mice, and that MCC950 further enhances the protective effects of H_2.

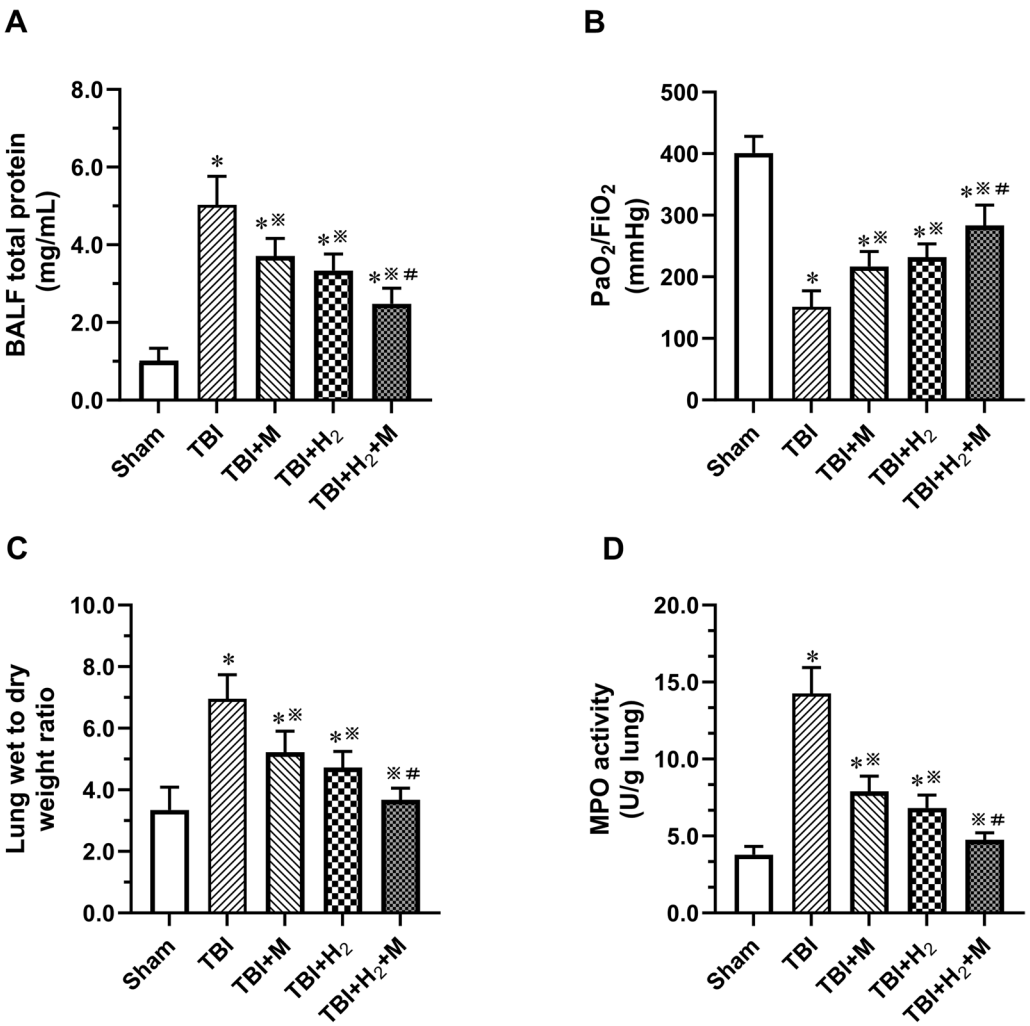

Fig. 2 Lung function deatection for H_2 and MCC950 treatment. **A** BALF total protein concentration; **B** PaO_2/FiO_2 ratio; **C** lung wet/dry weight ratio; **D** lung MPO activity. Values are expressed as mean ± standard deviation (n = 6). *P < 0.05 versus Sham group; ※P < 0.05 versus TBI group; #P < 0.05 versus TBI + H_2 group

2% H_2 treatment and MCC950 mitigated histopathological changes and apoptosis in lung tissues of TBI mice

We observed obvious lung injury in histopathological analysis of TBI group, including alveolar wall destruction, thickening, neutrophil infiltration in the interstitial and alveolar spaces, lung parenchymal edema and consolidation, and alveolar hemorrhage (Fig. 3A). Treatment with 2% H_2 gas and MCC950 mitigated these histopathological changes. Compare with other groups, the TBI + H_2 + M group showed the most substantial improvement in lung tissue morphology (Fig. 3C).

We also assessed the effects of 2% H_2 inhalation on affecting apoptosis in the lung tissues of TBI mice using TUNEL staining (Fig. 3B). The sham group exhibited minimal apoptosis, while the TBI group displayed numerous TUNEL-positive cells, indicating increasing apoptosis proportion (Fig. 3D). Apoptosis proportion significantly decreased through 2% H_2 treatment and MCC950. These findings indicate that 2% H_2 treatment effectively protect against apoptosis in TBI-induced ALI, and that MCC950 strengthened this protective capability. These were accordance with the histopathological observations across the groups.

To further explore relationships between effects of 2% H_2 treatment and inhibition of NLRP3 inflammasome activation, we conducted western blot analysis 24 h post-TBI or sham surgery (Fig. 4A–F). For TBI group, there was a significant increase in the expression levels of NLRP3, ASC, Caspase-1 p20, IL-18, and IL-1β, as well as in the gene expression levels of NLRP3, ASC, Caspase-1, IL-18, and IL-1β in lung tissues (Fig. 4G–K). However, 2% H_2 treatment reversed these increases. What's more, the NLRP3 inhibitor MCC950 hindered the expression of NLRP3, Caspase-1 p20, IL-18, and IL-1β, but not influenced related mRNA expression of NLRP3, ASC, Caspase-1, IL-18, and IL-1β.

To reveal positive effects of 2% H_2 treatment and MCC950, we detected the protein level changes of NLRP3 and Caspase-1. In Fig. 5A and B, the expression of NLRP3 and Caspase-1 significantly increased in TBI

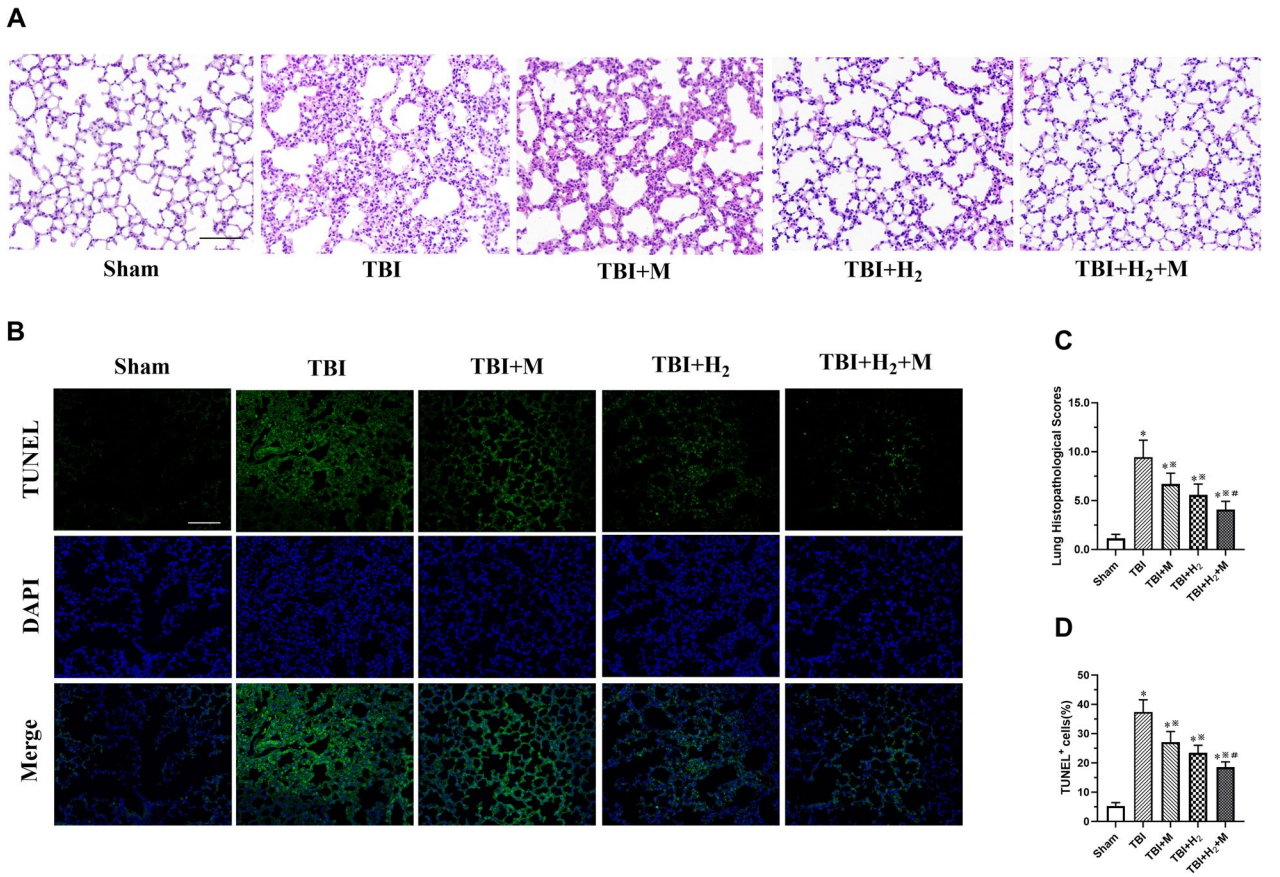

Fig. 3 Histopathological and apoptosis changes in lung tissues of 2% H_2 treatment and MCC950.. Scale bar = 100 μm. **A** H&E of lung tissue **C** quantitative analyses results of histopathological changes **B** TUNEL staining for apoptotic cells (green) and DAPI (blue) in lung tissues. **D** Quantitative data for cellular apoptosis in lung tissues. Scale bar = 100 μm. All values are presented as mean ± standard deviation (n = 6). *P < 0.05 versus Sham group; ※P < 0.05 versus TBI group; #P < 0.05 versus TBI + H_2 group

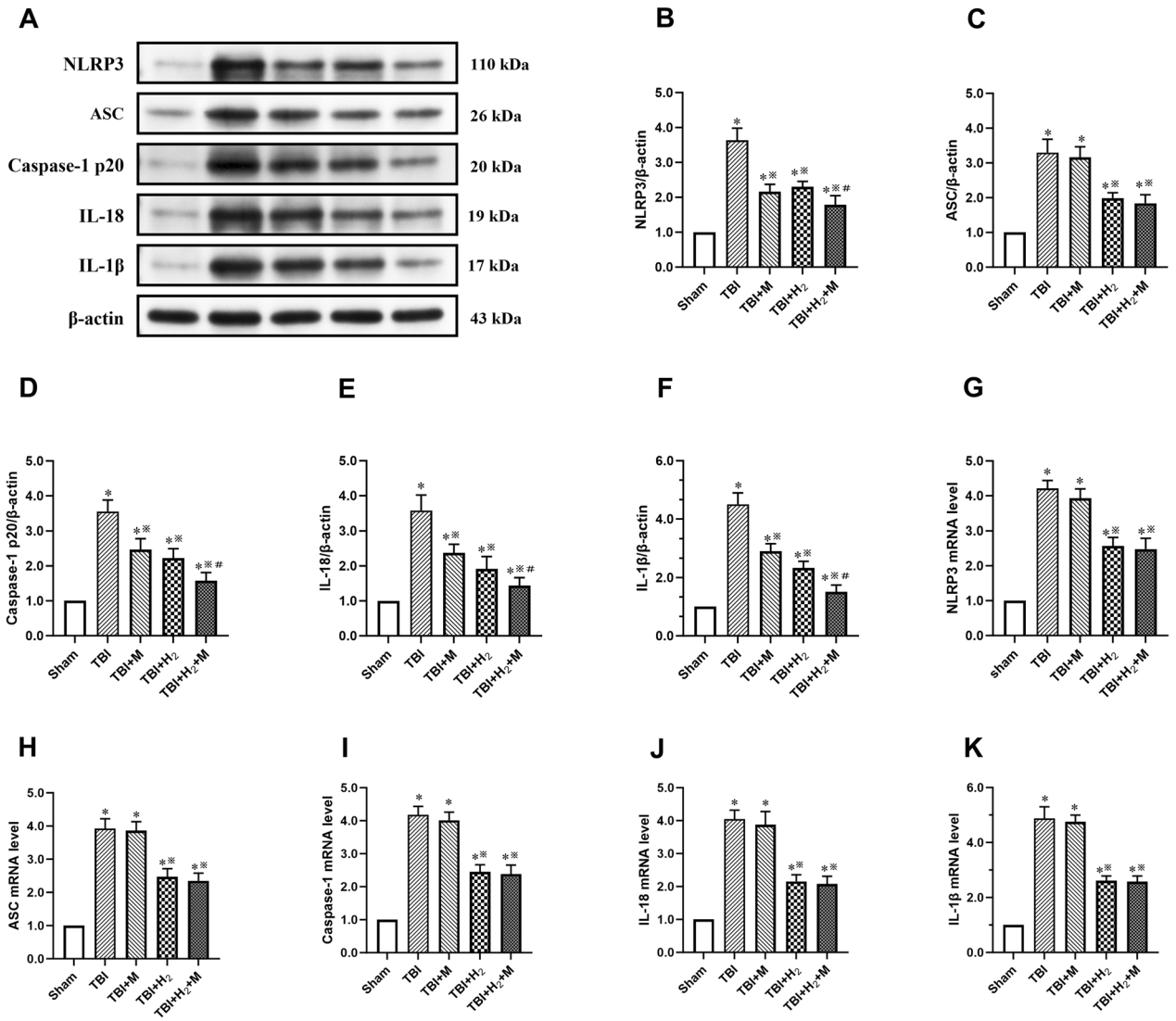

Fig. 4 NLRP3 inflammasome activation and related protein expression evaluation in lung tissues. **A** Western blot plot for proteins NLRP3 and related protein (**B**), ASC (**C**), caspase-1 p20 (**D**), IL-18 (**E**), and IL-1β (**F**) in lung tissues. qRT-PCR analysis of **G**–**I** NLRP3, ASC, Caspase-1 and, downstream IL-18 (**J**) and IL-1β (**K**). Values are presented as mean ± standard deviation (n = 3–5). *P < 0.05 versus Sham group; ※P < 0.05 versus TBI group; #P < 0.05 versus TBI + H_2 group

mice. Both 2% H_2 treatment and MCC950 were capable of inhibiting the expression of NLRP3 and Caspase-1. Notably, the integration application of MCC950 furtherly enhanced the protective effects of 2% H_2 treatment in TBI mice. Quantitative analysis of NLRP3 and Caspase-1 protein also supported above observations (Fig. 5C and D).

Discussion

Traumatic brain injury (TBI) constitutes a significant contributor to global morbidity and mortality rates. Patients with TBI often experience pulmonary complications, including ALI or ARDS, which are correlated with adverse clinical outcomes [21]. In addition, lung injury also can be induced by mild traumatic brain injury, and that has been underestimated [22]. The CCI model was classically used to establish a focal traumatic brain injury model [23]. It has been found that lung injury can occur 3 h after CCI operation, and it significantly aggravated at 24 h after CCI operation [1, 2]. Similarly, we showed obvious lung injury was induced at 24 h after CCI operation in this study.We observed that the concentration of H_2 in both arterial and venous quickly reached saturation during continuous inhalation and remained at

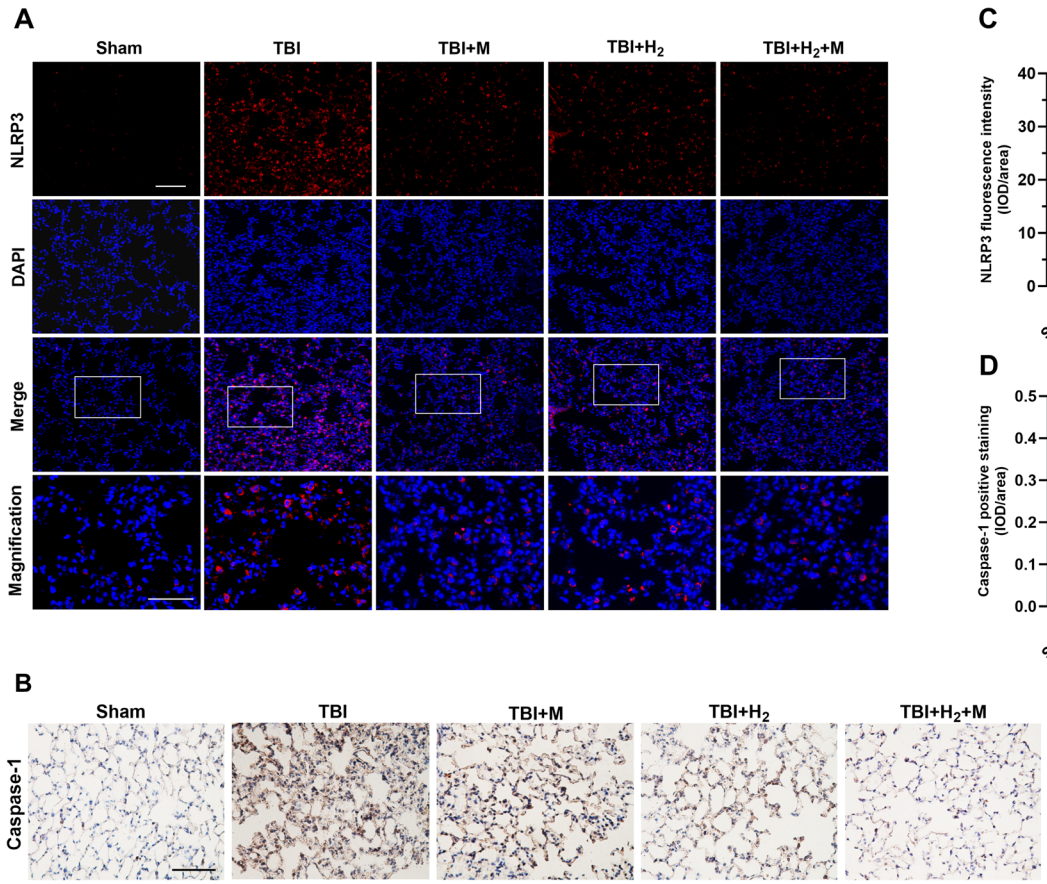

Fig. 5 NLRP3 and Casepase-1 expression and distribution in lung tissues. **A** Immunofluorescent staining for NLRP3 (red) and DAPI (blue). **B** Immunohistochemical staining for Caspase-1 (dark brown) and hematoxylin (blue). **C** Quantitative data of NLRP3 fluorescence intensity in the lung tissues. Scale bar = 100 μm; magnification, scale bar = 50 μm. **D** Quantitative data of Caspase-1 positive staining in the lung tissues. Scale bar = 100 μm. Values are presented as mean ± standard deviation (n = 5). *P < 0.05 versus Sham group; ※P < 0.05 versus TBI group; #P < 0.05 versus TBI + H_2 group

this saturated level for a period of time. This suggests that inhalation of H_2 can have direct and rapid effects on the lungs. The results of this study demonstrated that 2% H_2 treatment significantly reversed ALI and lung dysfunction in mice 24 h after TBI. There was a significant reduction in BALF total protein and PaO_2/FiO_2 ratio, lung wet/dry weight ratio, and lung MPO levels. Additionally, histopathological analysis showed marked alleviation of lung injury, indicating that 2% H_2 treatment effectively ameliorated lung damage following TBI.

There is a strong correlation between ALI, TBI, and neurogenic pulmonary edema (NPE), with NPE being a major cause of mortality among affected patients [24]. Inflammation plays a central role in the pathophysiology of ALI following TBI. TBI could trigger neuroinflammatory response to exacerbate secondary injury mechanisms. This type of inflammatory response is not only driven by peripheral immune mediators breaching a compromised blood–brain barrier, but also by a complex interaction between central and peripheral cellular components [25]. The inflammatory cascade, triggered by the release of pro-inflammatory cytokines, could ultimately result in cell death through various mechanisms [26].

The inflammasome as a key component of the innate immune system, has been implicated in the pro-inflammatory response in TBI field. Recent studies suggest that inflammasomes contribute to the development of lung injury after TBI [1]. Among the various inflammasomes, NLRP3 inflammasome is garnering attention as a promising target for therapeutic intervention. Excessive inflammation, driven by inflammasome activation, is central to the pathogenesis of post-traumatic conditions, including trauma-induced acute lung complications. This could lead to both systemic and localized activation of NLRP3, promoting caspase-1 and facilitating the maturation of pro-inflammatory cytokines such as IL-1β and IL-18 [27]. Recent research indicates that pharmacological agents,

such as dexmedetomidine, may offer neuroprotective effects by suppressing NF-κB and NLRP3 inflammasome activation, potentially mitigating acute post-traumatic inflammatory responses [22] Other studies have shown that H_2 inhalation can inhibit NLRP3 inflammasome activation and the TLR4/NF-κB signaling pathway, offering neuroprotection in models of subarachnoid hemorrhage [12].

Our findings revealed that TBI leads to upregulation of NLRP3 expression, which subsequently triggers ASC oligomerization and the recruitment of pro-Caspase-1, ultimately facilitated the assembly of the NLRP3 inflammasome complex in lung cells. This process activates Caspase-1. The release of these pro-inflammatory cytokines exacerbates the inflammatory response and induces apoptosis following traumatic brain injury (TBI). Furthermore, treatment with 2% H_2 significantly downregulates NLRP3 activation in mice with TBI-induced acute lung injury (ALI). These results demonstrated that 2% H_2 treatment may offer protective effects against ALI in the context of TBI by inhibiting NLRP3 inflammasome activation.

It is well established that inhibition of the NLRP3 inflammasome represents a promising strategy for the development of novel treatments for inflammatory diseases. MCC950, a potent and selective NLRP3 inhibitor, effectively suppresses NLRP3 activation, blocks ASC oligomerization, prevents the cleavage of pro-Caspase-1 into its active form (Caspase-1), and ultimately reduces Caspase-1-dependent pyroptosis and the production of IL-1β and IL-18 [23]. Recent studies have shown that MCC950 can repress NLRP3 inflammasome activation, highlighting its potential as a therapeutic strategy for TBI [24]. Our findings further demonstrated that MCC950 significantly decreased the expression and activation of NLRP3, but did not affect the expression of ASC or the mRNA levels of NLRP3, ASC, Caspase-1, IL-18, and IL-1β in lung tissues following TBI. These results suggest that combining 2% H_2 treatment with MCC950-induced repression of the NLRP3 inflammasome may offer a potential therapeutic approach for TBI-induced acute lung injury (ALI). However, our study had several limitations. Notably, we did not investigate the specific factors that induce NLRP3 inflammasome activation, nor did we explore the exact mechanisms by which H_2 interacts with the NLRP3 inflammasome or identify potential targets of H_2 on NLRP3. Additionally, we did not localize ASC protein in the lung, which would have provided further insight and enhanced the comprehensiveness of our study.

Conclusions

In conclusion, our study suggests that inhalation of 2% H_2 rapidly distributes throughout the body, maintaining elevated hydrogen concentrations in the blood for up to one hour. The protective effects of H_2 on lung injury in TBI mice are likely mediated through the inhibition of NLRP3 inflammasome activation, ultimately reducing inflammation and apoptosis. Based on these results, we propose that H_2 inhalation as a candidate safe and effective therapeutic strategy for preventing lung injury in TBI patients. It is of great potential for wide clinical application.

Acknowledgements
Not applicable.

Author contributions
Lingling Liu: writing—original draft, methodology, data curation. Shuzhi Wang: methodology, formal analysis, data curation. Lianhao Jiang: visualization, validation, software. Jiwei Wang: data curation, conceptualization, funding acquisition. Jun Chen: data curation, conceptualization. Hongtao Zhang: writing—review and editing, supervision. Yuanlin Wang: writing—review and editing, supervision.

Funding
This research was funded by the National Natural Science Foundation of Tianjin (Grant No. 20JCQNJC01270) and sponsored by Tianjin Health Research Project (TJWJ2022XK006).

Data availability
Data sharing is not applicable to this article as no datasets were generated or analysed during the current study.

Declarations

Ethics approval and consent to participate
All experimental got approved from the Animal Ethical and Welfare Committee of Tianjin Huanhu Hospital HHLL-2023-059.

Consent for publication
Not applicable.

Competing interests
The authors declare no competing interests.

Received: 20 March 2025 Accepted: 13 May 2025
Published online: 22 May 2025

References

1. Kerr NA, de Rivero Vaccari JP, Abbassi S, Kaur H, Zambrano R, Wu S, Dietrich WD, Keane RW. Traumatic brain injury-induced acute lung injury: evidence for activation and inhibition of a neural-respiratory-inflammasome axis. J Neurotrauma. 2018;35(17):2067–76.
2. Liu Y, Li F, Tang L, Pang K, Zhang Y, Zhang C, Guo H, Ma T, Zhang X, Yang G, et al. Extracellular mitochondria contribute to acute lung injury via disrupting macrophages after traumatic brain injury. J Neuroinflamm. 2025;22(1):63.
3. Kerr NA, de Rivero Vaccari JP, Umland O, Bullock MR, Conner GE, Dietrich WD, Keane RW. Human lung cell pyroptosis following traumatic brain injury. Cells. 2019;8(1):69.
4. Ziaka M, Exadaktylos A. Brain-lung interactions and mechanical ventilation in patients with isolated brain injury. Crit Care. 2021;25(1):358.

5. Matin N, Sarhadi K, Crooks CP, Lele AV, Srinivasan V, Johnson NJ, Robba C, Town JA, Wahlster S. Brain-lung crosstalk: management of concomitant severe acute brain injury and acute respiratory distress syndrome. Curr Treat Options Neurol. 2022;24(9):383–408.
6. Robba C, Asgari S, Gupta A, Badenes R, Sekhon M, Bequiri E, Hutchinson PJ, Pelosi P, Gupta A. Lung injury is a predictor of cerebral hypoxia and mortality in traumatic brain injury. Front Neurol. 2020;11:771.
7. Johnsen HM, Hiorth M, Klaveness J. Molecular hydrogen therapy—a review on clinical studies and outcomes. Molecules. 2023;28(23):7785.
8. Wu C, Zou P, Feng S, Zhu L, Li F, Liu TC, Duan R, Yang L. Molecular hydrogen: an emerging therapeutic medical gas for brain disorders. Mol Neurobiol. 2023;60(4):1749–65.
9. Liu L, Xie K, Chen H, Dong X, Li Y, Yu Y, Wang G, Yu Y. Inhalation of hydrogen gas attenuates brain injury in mice with cecal ligation and puncture via inhibiting neuroinflammation, oxidative stress and neuronal apoptosis. Brain Res. 2014;1589:78–92.
10. Yu Y, Yang Y, Yang M, Wang C, Xie K, Yu Y. Hydrogen gas reduces HMGB1 release in lung tissues of septic mice in an Nrf2/HO-1-dependent pathway. Int Immunopharmacol. 2019;69:11–8.
11. Li Y, Li Q, Chen H, Wang T, Liu L, Wang G, Xie K, Yu Y. Hydrogen gas alleviates the intestinal injury caused by severe sepsis in mice by increasing the expression of heme oxygenase-1. Shock. 2015;44(1):90–8.
12. Wang L, Zhao C, Wu S, Xiao G, Zhuge X, Lei P, Xie K. Hydrogen gas treatment improves the neurological outcome after traumatic brain injury via increasing miR-21 expression. Shock. 2018;50(3):308–15.
13. Cai L, Gong Q, Qi L, Xu T, Suo Q, Li X, Wang W, Jing Y, Yang D, Xu Z, et al. ACT001 attenuates microglia-mediated neuroinflammation after traumatic brain injury via inhibiting AKT/NFκB/NLRP3 pathway. Cell Commun Signal. 2022;20(1):56.
14. Zhuang K, Zuo YC, Sherchan P, Wang JK, Yan XX, Liu F. Hydrogen inhalation attenuates oxidative stress related endothelial cells injury after subarachnoid hemorrhage in rats. Front Neurosci. 2019;13:1441.
15. Zhou H, Zhang Q, Huang W, Zhou S, Wang Y, Zeng X, Wang H, Xie W, Kong H. NLRP3 inflammasome mediates silica-induced lung epithelial injury and aberrant regeneration in lung stem/progenitor cell-derived organotypic models. Int J Biol Sci. 2023;19(6):1875–93.
16. Zhou L, Wang X, Xue W, Xie K, Huang Y, Chen H, Gong G, Zeng Y. Beneficial effects of hydrogen-rich saline against spinal cord ischemia-reperfusion injury in rabbits. Brain Res. 2013;1517:150–60.
17. Shahror RA, Linares GR, Wang Y, Hsueh SC, Wu CC, Chuang DM, Chiang YH, Chen KY. Transplantation of mesenchymal stem cells overexpressing fibroblast growth factor 21 facilitates cognitive recovery and enhances neurogenesis in a mouse model of traumatic brain injury. J Neurotrauma. 2020;37(1):14–26.
18. Di Pietro C, Öz HH, Zhang PX, Cheng EC, Martis V, Bonfield TL, Kelley TJ, Jubin R, Abuchowski A, Krause DS, et al. Recruitment of monocytes primed to express heme oxygenase-1 ameliorates pathological lung inflammation in cystic fibrosis. Exp Mol Med. 2022;54(5):639–52.
19. Cao F, Tian X, Li Z, Lv Y, Han J, Zhuang R, Cheng B, Gong Y, Ying B, Jin S, et al. Suppression of NLRP3 inflammasome by erythropoietin via the EPOR/JAK2/STAT3 pathway contributes to attenuation of acute lung injury in mice. Front Pharmacol. 2020;11:306.
20. Peng Y, Wu Q, Tang H, Chen J, Wu Q, Yuan X, Xiong S, Ye Y, Lv H. NLRP3 regulated CXCL12 expression in acute neutrophilic lung injury. J Inflamm Res. 2020;13:377–86.
21. Della Torre V, Badenes R, Corradi F, Racca F, Lavinio A, Matta B, Bilotta F, Robba C. Acute respiratory distress syndrome in traumatic brain injury: how do we manage it? J Thorac Dis. 2017;9(12):5368–81.
22. Humphries DC, O'Neill S, Scholefield E, Dorward DA, Mackinnon AC, Rossi AG, Haslett C, Andrews PJD, Rhodes J, Dhaliwal K. Cerebral concussion primes the lungs for subsequent neutrophil-mediated injury. Crit Care Med. 2018;46(9):e937–44.
23. Ge X, Zhu L, Li M, Li W, Chen F, Li Y, Zhang J, Lei P. A novel blood inflammatory indicator for predicting deterioration risk of mild traumatic brain injury. Front Aging Neurosci. 2022;14: 878484.
24. Bai W, Zhu WL, Ning YL, Li P, Zhao Y, Yang N, Chen X, Jiang YL, Yang WQ, Jiang DP, et al. Dramatic increases in blood glutamate concentrations are closely related to traumatic brain injury-induced acute lung injury. Sci Rep. 2017;7(1):5380.
25. Kerr N, de Rivero Vaccari JP, Dietrich WD, Keane RW. Neural-respiratory inflammasome axis in traumatic brain injury. Exp Neurol. 2020;323: 113080.
26. Wang Y, Wang C, Zhang D, Wang H, Bo L, Deng X. Dexmedetomidine protects against traumatic brain injury-induced acute lung injury in mice. Med Sci Monit. 2018;24:4961–7.
27. Bortolotti P, Faure E, Kipnis E. Inflammasomes in tissue damages and immune disorders after trauma. Front Immunol. 1900;2018:9.

Publisher's Note